Journal of The Electrochemical Society

Partially Oxidized Tantalum Carbonitrides as a New Nonplatinum Cathode for PEFC–1–

Journal of The Electrochemical Society, **155** (4) B400-B406 (2008)
0013-4651/2008/155(4)/B400/7/$23.00 © The Electrochemical Society

Partially Oxidized Tantalum Carbonitrides as a New Nonplatinum Cathode for PEFC–1–

A. Ishihara,[z] Y. Shibata, S. Mitsushima,[*] and K. Ota[*]

Chemical Energy Laboratory, Yokohama National University, Yokohama 240-8501, Japan

Partially oxidized $TaC_{0.58}N_{0.42}$ has been investigated as a cathode for polymer electrolyte fuel cells (PEFCs). Catalytic activity for the oxygen reduction reaction (ORR) significantly depends on the oxidation state of $TaC_{0.58}N_{0.42}$. $TaC_{0.58}N_{0.42}$ and Ta_2O_5 had a poor catalytic activity for the ORR. The onset potential on the partially oxidized $TaC_{0.58}N_{0.42}$ for the ORR had a maximum value of 0.83 V vs a reversible hydrogen electrode in 0.1 mol dm^{-3} H_2SO_4 at 30°C. X-ray diffraction analysis showed that the specimens, which had a definite catalytic activity for the ORR, had both TaC_xN_y and Ta_2O_5 peaks. This result indicated that an appropriate oxidation of the $TaC_{0.58}N_{0.42}$ was essential to enhance the catalytic activity for the ORR.
 [DOI: 10.1149/1.2839606]

Manuscript submitted September 5, 2007; revised manuscript received December 27, 2007.
Available electronically February 20, 2008.

Polymer electrolyte fuel cells (PEFCs) are expected as power sources for residential and transport applications due to their high theoretical efficiency of energy conversion, high power density, and low operating temperature. However, PEFCs have some serious problems to be solved before wide commercialization. In particular, a large overpotential of oxygen reduction reaction (ORR) must be reduced in order to obtain high energy efficiency. Although Pt is generally used as a cathode catalyst in the present PEFCs, its catalytic activity for the ORR is insufficient to obtain the required efficiency.[1,2] Other issues regarding Pt use are its high cost and limited resources. Considering an application to fuel cell vehicles, the natural resource of Pt is insufficient. Therefore, many attempts, such as a greater dispersion of Pt particles and/or an alloying with transition metals, have been made to reduce Pt utilization. However, because dissolution of highly dispersed Pt particles and oxidation of a support carbon became important issues for long-time operation in recent years, a drastic reduction of the Pt utilization seemed difficult. Therefore, development of a stable nonplatinum catalyst is vital.[3,4]

Many studies have been performed to develop nonplatinum cathode catalysts for low-temperature fuel cells. Organometallic complexes and chalcogenides were famous as candidates for the alternative Pt catalysts. Jasinski first introduced a cobalt phthalocyanine as an electrocatalyst for the ORR in 35% KOH (potassium hydroxide) in 1964.[5] Jahnke and Schönborn applied transition metal phthalocyanines to the non-Pt cathode catalysts in 4.5 N H_2SO_4 in 1969.[6] Many organometallic complexes have been widely investigated since then. Molecular design of the organometallic complexes is easier than that of metal-based catalysts. Mononuclear cobalt porphrins[7] and iron porphrins[8] reduced O_2 to H_2O_2 because an O_2 molecule interacted with one metal center in an end-on position. Dicobalt cofacial porphyrins were able to promote a direct reduction of O_2 to H_2O through a four-electron mechanism in acidic media where an O_2 molecule coordinated to form a μ-O_2 bridge between the two cobalt centers, allowing subsequent scission of the O–O bond.[9] Their results revealed that geometry of porphyrins was very important for the efficient electron transfer and cleavage of the O–O bond. In addition, Jahnke et al.[10] found in the 1970s that heat-treatment of organometallic materials in an inert gas atmosphere enhanced their catalytic activity and stability. Many researchers, such as Yeager and Scherson et al.,[11,12] Van der Putten et al.,[13,14] Van Veen and Bouwkamp-Wijnoltz et al.,[15,16] and Gruenig and Wiesener,[17,18] etc., have proposed several models to explain the enhancement effect.

Alonso-Vante et al. found that $Mo_{4.2}Ru_{1.8}Se_8$ had a superior catalytic activity for the ORR in acidic media in 1986.[19] Extended X-ray absorption fine structure analysis revealed that an O_2 molecule adsorbed on Mo, Ru acted as an active center, and Se affected an electronic state and a local structure of Ru.[20] RuSe, RuTe, MoReSe, MoRhS, MoOsS, MoSe, ReRuS, IrRuS, (RuMo)SeO, WRuSe, RhS, RhSe, RuCrSe, RuFeSe, and CoSe were investigated besides MoRuSe. Because these chalcogenides were inactive for methanol, the development for cathodes as direct methanol fuel cells was examined. However, these catalysts have neither a sufficient electrocatalytic activity for the ORR nor a long-term stability.

We have reported that tungsten carbide with tantalum addition,[21] tantalum oxynitride powder,[22,23] zirconium oxide,[24,25] titanium oxide,[26] zirconium oxynitride,[27] chromium carbonitride,[28] and tantalum carbonitride[29] were stable in an acid solution and had a definite catalytic activity for the ORR. We found that oxide-based Zr compounds with oxygen defects on the surface had a definite catalytic activity for the ORR.[27] Because ZrO_2 had a wide bandgap, 5.3 eV,[30] the oxidation state of the surface on the oxide-based Zr compounds had to be controlled. Tantalum (Ta_2O_5), having the highest oxidation state, had a wide bandgap of 4.3 eV, and the upper energy level of the valence band is 3.4 V vs a standard hydrogen electrode (SHE).[30] The rate of a redox reaction depends on the product of the state density of electrons in the electrode and that of electrons in the reductant and oxidant particles near the Fermi level.[31] Because the upper energy level of the valence band in Ta_2O_5 is far from the Fermi level of Ta_2O_5, ca. 0 V vs SHE,[32] the ORR hardly proceeds on the Ta_2O_5. Therefore, it is necessary to change the state density of electrons in the Ta_2O_5 with the addition of other elements and/or introduction of some surface defects. We used tantalum carbonitride (TaC_xN_y) powder as a starting material, and a partial oxidation of the starting material was performed to control the oxidation state of the catalyst. Tantalum carbonitride consists of TaC and TaN. Both TaC and TaN have the same crystalline structure (rock-salt type) and form a complete solid solution to compose TaC_xN_y. TaC and TaN are electrical conductors: TaC 4×10^4 S cm^{-1}; TaN 4–7 $\times 10^3$ S m^{-1}.[33] The band structure of TaC is characterized by overlapping C 2p and Ta 5d bands.[34] The Fermi level lies slightly above the minimum of the density of states of the band,[34] indicating that TaC shows metallic behavior. In the case of TaN, the band structure is fundamentally similar to that of TaC.[35] Therefore, the electronic structure of TaC_xN_y changes consecutively with the substitution of C atoms for N atoms.[36] A partial oxidation, that is, the substitution for O atoms, brings an increasing ionic component of the chemical bonding, because the energy difference between the Ta 5d and O 2p orbitals is higher than that between Ta 5d and C or N 2p.

A sufficient electrical contact between an oxide-based catalyst and a current collector is very important to obtain a large reaction current. In the present study, in order to control the oxidation state and to obtain the sufficient electrical contact between the catalysts and the current collector, two methods have been tried to prepare the working electrode. First, electrophoretic deposition of a starting material was performed using a titanium plate as a current collector.

* Electrochemical Society Active Member.
[z] E-mail: a-ishi@ynu.ac.jp

After the electrophoretic deposition of the tantalum carbonitride powders on the Ti plate, a partial oxidation was performed with heat-treatment in the temperature range from 600 to 1400°C under flowing 2% H_2/N_2 gas containing 0.25% oxygen. Second, the tantalum carbonitride powders were partially oxidized and then mixed with carbon black to obtain a sufficient electrical contact. The mixed powder was dropped onto a glassy carbon rod and covered by recast Nafion.

Experimental

Tantalum carbonitride (TaC_xN_y) powder was used as a starting material. Ta_2O_5 powder and carbon black were uniformly mixed, and the mixture was heat-treated at 1600°C under flowing N_2 to make carbonitride. The composition of the TaC_xN_y was controlled by the quantity of carbon black. In the present study, $TaC_{0.58}N_{0.42}$ powder was used as a starting material.

Working electrodes were prepared using two methods. First, an electrophoretic deposition method[37] was used. The $TaC_{0.58}N_{0.42}$ powder (100 mg) was suspended in 50 cm^3 of acetone containing 10 mg of I_2 with ultrasonic treatment. A titanium plate (10 × 10 mm) was used as a substrate. A counter electrode was an Au plate. An electrophoretic deposition of the $TaC_{0.58}N_{0.42}$ on the Ti plate was performed as a cathode with an applied potential of 100 V for 60 s. The $TaC_{0.58}N_{0.42}$/Ti specimen was then heated in an alumina tube furnace (KT-3 × 14-VP, Koyo Thermo Systems) under flowing H_2/N_2 gas (H_2 2%) containing 0.25% oxygen in the temperature range from 600 to 1400°C for 1 h. Because the H_2/N_2 gas contained 0.25% oxygen, the $TaC_{0.58}N_{0.42}$ on the Ti plate was partially oxidized during the heat-treatment. Hydrogen in the flowing gas restrained the fast oxidation of the $TaC_{0.58}N_{0.42}$ to easily control the degree of oxidation. The color of the powder on the Ti substrate gradually changed from dark brown to gray at a higher heat-treatment temperature.

Second, the tantalum carbonitride powders were heat-treated at 1200°C for 10 h under different flow rates of the 2% H_2/N_2 gas containing 0.25% oxygen to obtain powder specimens with different oxidation states. A partially oxidized specimen was mixed with carbon black, Ketjen Black (5 wt %), and the mixed powder (2.8 mg cm^{-2}) was dropped onto a glassy carbon rod (Φ = 5.2 mm). A 0.5 wt % Nafion solution was then dropped onto the surface to cover the mixed powder. In addition, in order to examine the effect of the mixture with the carbon, a partially oxidized powder was dropped onto the glassy carbon rod without carbon black.

All electrochemical experiments were conducted in a three-electrode cell under nitrogen or oxygen atmosphere in 0.1 mol dm^{-3} H_2SO_4 at 30°C. A reference electrode was a reversible hydrogen electrode (RHE) in the same solution. Cyclic voltammetry (scan rate 50 mV s^{-1}, 0.05–1.0 V) was performed under nitrogen atmosphere to investigate an electrochemical stability of the specimens. Slow scan voltammetry (scan rate 5 mV s^{-1}, 1.0–0.2 V) was performed under nitrogen or oxygen atmosphere to evaluate catalytic activity for the ORR. A current difference between under O_2 and under N_2 might be due to the oxygen reduction. Therefore, the oxygen reduction current density (i_{ORR}) was defined as the difference in the current densities between the area under the O_2 atmosphere (i_{O_2}) and the N_2 atmosphere (i_{N_2}). The current density was based on the geometric surface area of the working electrode.

The crystalline structure of the specimens was analyzed using X-ray diffraction (XRD; XRD-6000, Shimadzu) with Cu Kα radiation. The cross-sectional surface of the interface between the catalyst powder and the Ti substrate was etched with a cross-section polisher (CP, JEOL), and the $TaC_{0.58}N_{0.42}$ powder with and without heat-treatment, was observed using a scanning electron microscope (SEM) (JSM-7000F, JEOL). X-ray photoelectron spectroscopy (XPS; Axis-Nova, Kratos) was performed to reveal the chemical bonding state of the specimens. The ionization potential of partially oxidized $TaC_{0.58}N_{0.42}$ was measured using a photoelectron spectrometer surface analyzer (model AC-2, Riken Keiki).[38]

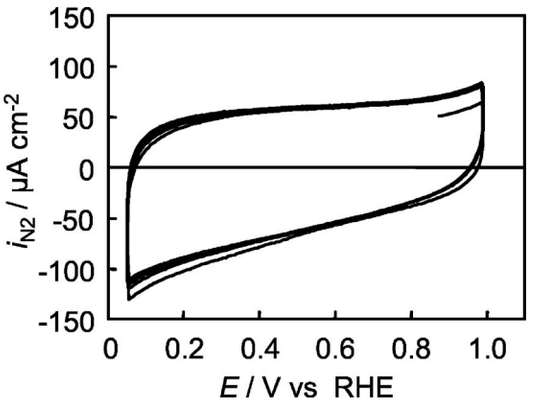

Figure 1. CV of $TaC_{0.58}N_{0.42}$/Ti heat-treated at 1000°C in 0.1 mol dm^{-3} H_2SO_4 at 30°C under N_2 atmosphere. Scan rate: 50 mV s^{-1}.

Results and Discussion

Partially oxidized $TaC_{0.58}N_{0.42}$ on a titanium plate.— Figure 1 shows the cyclic voltammogram (CV) of the $TaC_{0.58}N_{0.42}$/Ti which was heat-treated at 1000°C in 0.1 mol dm^{-3} sulfuric acid at 30°C under N_2 atmosphere. The shape of the CV hardly changed after several potential cycles. No specific peak due to an anodic dissolution was observed in the CV. Because the shapes of the CVs in the first potential scan and the steady state were almost the same, the surface of the specimens after heating at 1000°C was stable. In addition, an anodic and a cathodic electric charge in the steady state CV in Fig. 1 were calculated to be 1.13 and 1.14 mC cm^{-2}, respectively. These values agree well with each other. Therefore, these charges were due to a charge and a discharge of a double layer, indicating that no one-sided reaction occurred. The CVs of the specimens heat-treated at other temperatures also reached a steady state immediately. Figure 2 shows the relationship between the anodic and cathodic electric charges calculated from the steady-state CVs of the specimens with various heat-treatment temperatures. A linear relation was obtained in Fig. 2. The anodic electric charges were always equal to the cathodic charges in each specimen. Therefore, both electrical charges were responsible for the charge and discharge of the electric double layer. These results revealed that the $TaC_{0.58}N_{0.42}$/Ti with the heat-treatment had a high electrochemical stability in acidic solution. The charge increased with the heat-treatment temperature up to 1000°C, and then decreased. Assuming that a real surface area is proportional to the charge of the electric double layer, the specimen heat-treated at 1000°C had the highest real surface area in the present work.

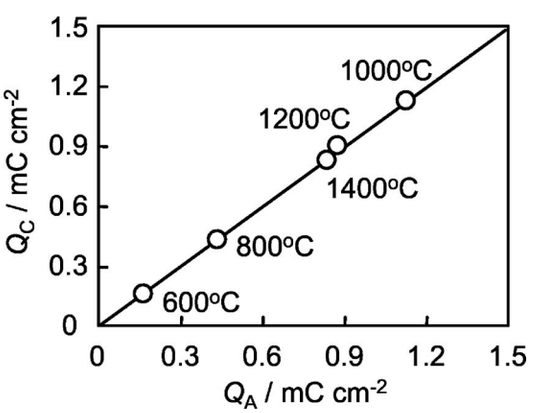

Figure 2. Relationship between the anodic and the cathodic electric charge of $TaC_{0.58}N_{0.42}$/Ti heat-treated in the range 600–1400°C.

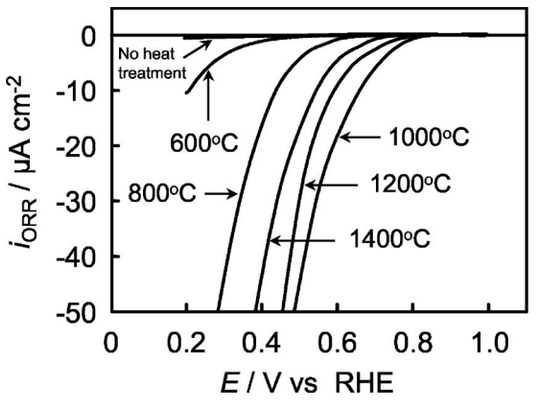

Figure 3. Potential–i_{ORR} curves for the ORR of $TaC_{0.58}N_{0.42}$/Ti with and without heat-treatment in 0.1 mol dm^{-3} H_2SO_4 at 30°C with a scan rate of 5 mV s^{-1}.

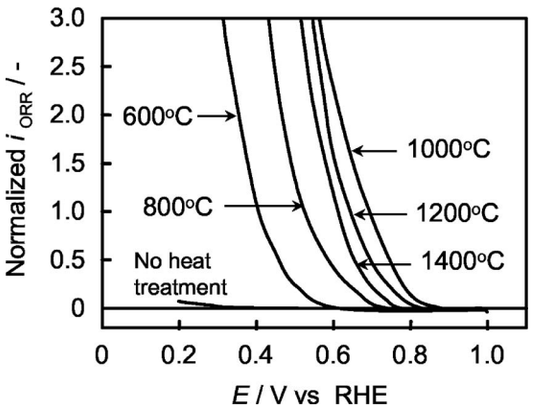

Figure 5. Potential-normalized oxygen reduction current of $TaC_{0.58}N_{0.42}$/Ti with and without heat-treatment in 0.1 mol dm^{-3} H_2SO_4 at 30°C with a scan rate of 5 mV s^{-1}.

Figure 3 shows the potential–current density curves for the ORR (i_{ORR}) on the $TaC_{0.58}N_{0.42}$/Ti, with and without heat-treatment, in the range from 600 to 1400°C in 0.1 mol dm^{-3} H_2SO_4 at 30°C with a scan rate of 5 mV s^{-1}. No anodic current was observed in all specimens up to 1.0 V vs RHE. Because the ORR currents of the specimens with heat-treatment at 600°C and without heat-treatment were observed below 0.5 V, these specimens had a poor catalytic activity for the ORR. The oxygen reduction current and the onset potential of the ORR increased with the increase in heat-treatment temperature up to 1000°C, and then decreased. This result indicates that the catalytic activity for the ORR significantly depends on the heat-treatment temperature. Figure 4 shows the dependence of the electrode potential at the i_{ORR} of −0.2 μA cm^{-2}, that is, the onset potential for the ORR, and i_{ORR} at 0.4 V on heat-treatment temperature. The i_{ORR} at 0.4 V abruptly increased above 600°C, and the specimen heat-treated at 1000°C showed the highest activity for the ORR. Above 1000°C, the i_{ORR} sharply decreased. The onset potential on the specimen heat-treated at 1000°C was 0.81 V. The tendency of the decrease in the onset potential for the ORR above 1000°C was smaller than that of the decrease in the i_{ORR} at 0.4 V. Although the ORR proceeded at near 0.8 V on the specimens heat-treated at 1200 and 1400°C, the i_{ORR} at 0.4 V on these specimens was much smaller than that at 0.4 V on the specimen heat-treated at 1000°C. This result suggested that the electrical contact between the catalysts and the current collector (Ti plate) was insufficient at higher heat-treatment temperature. However, the heat-treatment at around 1000°C under 0.25% oxygen was found to be very useful to increase the catalytic activity for the ORR.

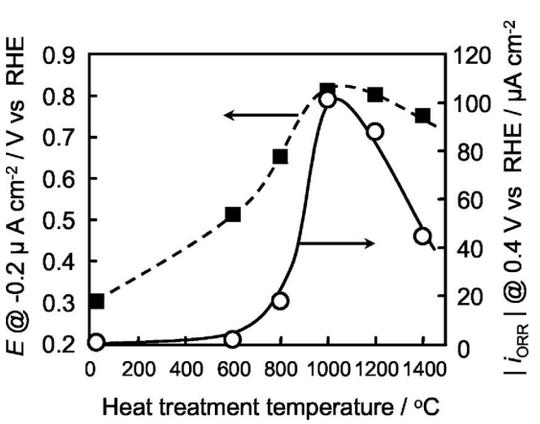

Figure 4. Dependence of E at −0.2 μA cm^{-2} and $|i$ORR$|$ at 0.4 V vs RHE on the heat-treatment temperature.

It is necessary to evaluate the real surface area, because the ORR current could increase due to the increase in real surface area of the specimen. The real surface area can be compared with the charge and discharge currents which are observed under the nitrogen atmosphere with a potential scan, assuming that the real surface area is proportional to the charge and discharge currents. Therefore, a normalized i_{ORR} was defined as the following equation using the current density observed under N_2 (i_{N_2})

$$\text{Normalized } i_{ORR}(E) = i_{ORR}(E)/i_{N_2}(E) \quad [1]$$

where (E) means the current at the potential of E. Needless to say, the normalized i_{ORR} was dependent on the electrode potential, because both i_{ORR} and i_{N_2} were dependent on the potential. An i_{N_2} was proportional to the real surface area determined by the surface state at a given potential. Therefore, the division of i_{ORR} by i_{N_2}, that is, normalized i_{ORR}, showed the reaction rate of the ORR with consideration of the effect of the real surface area. Figure 5 shows the potential—normalized i_{ORR} of $TaC_{0.52}N_{0.48}$/Ti with and without heat-treatment in 0.1 mol dm^{-3} H_2SO_4 at 30°C with a scan rate of 5 mV s^{-1}. The normalized i_{ORR} increased with the increase in heat-treatment temperature up to 1000°C and then decreased. This tendency corresponded to that of the i_{ORR} value. Therefore, the increase in i_{ORR} was due to the increase in the catalytic activity for the ORR. As a result, the heat-treatment enhanced the catalytic activity for the ORR, and the specimen heat-treated at 1000°C had the highest catalytic activity for the ORR.

Next, characterization of the specimens was performed in order to investigate the parameters affecting the catalytic activity for the ORR. Figure 6 shows the XRD patterns of the $TaC_{0.58}N_{0.42}$/Ti, with and without heat-treatment at 600–1400°C. An intensity of each specimen was normalized using the maximum peak of each pattern. Both TaC and TaN have the same crystalline structure (rock-salt type) and form a complete solid solution. The XRD pattern did not change from TaC (JCPDS: 35–0801) to TaN (JCPDS: 32–1283), and each peak shifts to a higher angle with the increase in nitrogen content, which is known as Vegard's law. In the present paper, the compounds with XRD peaks which existed between TaC and TaN were expressed as TaC_xN_y. In Fig. 6, the specimens with heat-treatment below 800°C had only TaC_xN_y (cubic) peaks. The oxidation into the bulk did not proceed below 800°C. The XRD patterns of Ta_2O_5 were observed above 1000°C. The peak intensity of the Ta_2O_5 increased with the increase in heat-treatment temperature above 1000°C, while the intensity of the TaC_xN_y decreased. The

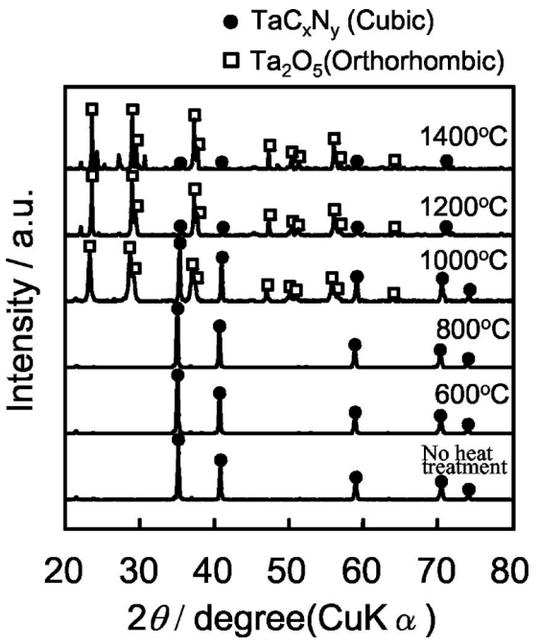

Figure 6. XRD patterns of $TaC_{0.58}N_{0.42}$/Ti, with and without heat-treatment.

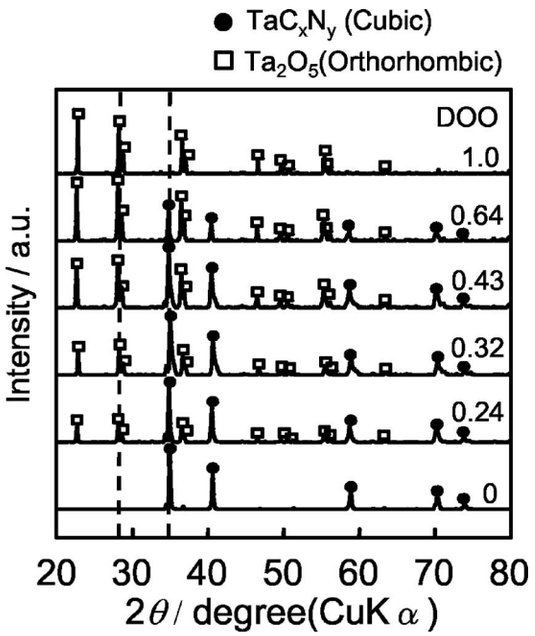

Figure 8. XRD patterns of $TaC_{0.58}N_{0.42}$, partially oxidized $TaC_{0.58}N_{0.42}$, and Ta_2O_5 powder.

crystalline structure gradually changed from TaC_xN_y to Ta_2O_5, and the color tone changed from dark brown to gray with the increase in heat-treatment temperature. Therefore, $TaC_{0.58}N_{0.42}$/Ti was partially oxidized during the heat-treatment due to the small amount of O_2. Because the partial oxidation proceeded at higher temperature, it is likely that the surface of the TaC_xN_y particles was oxidized with the remaining TaC_xN_y in the bulk. The highest activity for the ORR was obtained on the $TaC_{0.58}N_{0.42}$/Ti, which was heat-treated at 1000°C, and the diffraction peaks of both TaC_xN_y and Ta_2O_5 were observed in the specimen. Therefore, an appropriate oxidation might be required to have a definite catalytic activity for the ORR.

Figure 7 shows the cross-sectional SEM images of the $TaC_{0.58}N_{0.42}$ catalyst layer and the Ti substrate at 800, 1000, and 1200°C. The lower part of each image is the Ti substrate, and the upper part is the catalyst layer of the partially oxidized $TaC_{0.58}N_{0.42}$. The thickness of the catalyst layer was approximately 15–20 μm. The catalyst layer of each specimen was relatively uniform. The catalyst layer was very porous and the boundary between the substrate and the catalyst layer was distinct in the specimen which was heat-treated at 800°C. The catalyst layer became dense and the boundary became indistinct in the specimens which were heat-treated above 1000°C. The contact between the catalyst near the titanium plate side and the titanium plate were improved at higher temperature. However, it is thought that the contact of the catalyst powders near the surface side was deteriorated due to the progress of the oxidation. In addition, it is possible that new compounds containing titanium have a clear catalytic activity for the ORR. The effect of the Ti plate must be eliminated in order to determine the factors which affect the catalytic activity of the ORR.

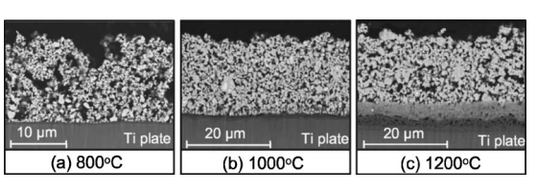

Figure 7. Cross-sectional SEM images of partially oxidized $TaC_{0.58}N_{0.42}$/Ti heat-treated at 800, 1000, and 1200°C.

Partially oxidized $TaC_{0.58}N_{0.42}$ mixed with carbon black on a glassy carbon rod.— In order to eliminate the effect of the Ti plate, the tantalum carbonitride powders were partially oxidized and then mixed with carbon black to obtain a sufficient electrical conductivity of the catalyst powder. The mixed powder was dropped onto a glassy carbon rod with a covering of recast Nafion.

In order to quantify the degree of oxidation of the $TaC_{0.58}N_{0.42}$, the peak intensity at $2\theta = 35°$ of TaC_xN_y (1 0 0), which was expressed as $I(TaC_xN_y)$, and the peak intensity at $2\theta = 28.3°$ of Ta_2O_5 orthorhombic (1 11 0), which was expressed as $I(Ta_2O_5)$, were utilized to calculate the ratio, $I(Ta_2O_5)/[I(TaC_xN_y) + I(Ta_2O_5)]$. The ratio, $I(Ta_2O_5)/[I(TaC_xN_y) + I(Ta_2O_5)]$ was designated as the degree of oxidation of the $TaC_{0.58}N_{0.42}$ and is expressed as DOO (degree of oxidation). Figure 8 shows the XRD patterns of the powder specimens with the different DOO. The DOO of the specimen with no heat-treatment was zero, that is, $TaC_{0.58}N_{0.42}$. Although the surface of the $TaC_{0.58}N_{0.42}$ was probably oxidized, no peaks of Ta_2O_5 were observed because the surface oxide layer was very thin. The DOO of the completely oxidized specimen was unity, that is, Ta_2O_5. However, this completely oxidized powder was not prepared using the heat-treatment in the present paper because of the low oxygen concentration and the short holding time. Therefore, a commercial reagent, Ta_2O_5 (Junsei Kagaku), was used as the powder with DOO of unity.

Figure 9 shows the SEM images of specimens with the DOO of 0 and 0.64. The particle size of the starting material (DOO = 0) was

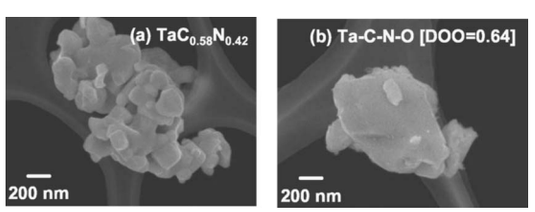

Figure 9. SEM images of (a) $TaC_{0.58}N_{0.42}$ and (b) partially oxidized $TaC_{0.58}N_{0.42}$ [DOO = 0.64] powder.

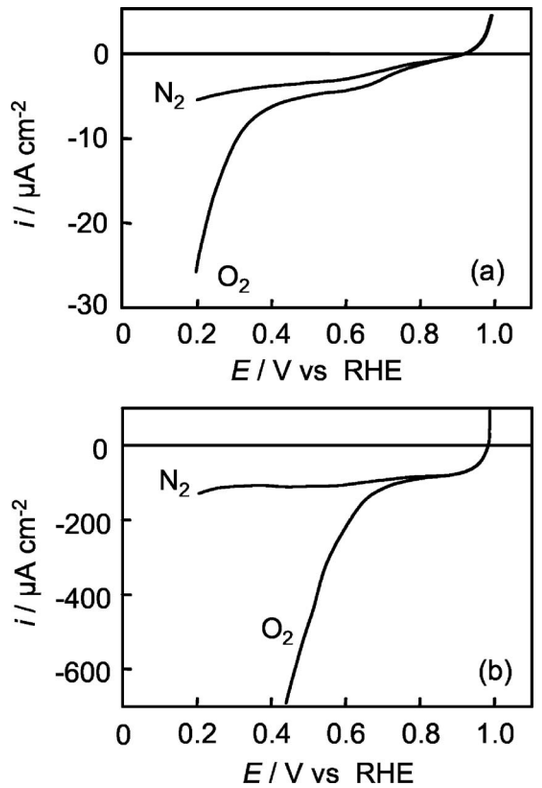

Figure 10. Effect of the mixture of the partially oxidized $TaC_{0.58}N_{0.42}$ (DOO = 0.43) with carbon black on the potential–current curves under N_2 and O_2: (a) no addition of carbon black and (b) mixture with carbon black, 0.1 mol dm^{-3} H_2SO_4, 30°C, 5 mV s^{-1}, N_2 and O_2

several hundreds of nanometers. The particle size of the partially oxidized specimen was larger than that of the starting materials due to the heat-treatment.

The electrical conductivity presumably decreased with the partial oxidation of the $TaC_{0.58}N_{0.42}$. Therefore, the mixture with carbon black was examined to increase the conductivity. Figure 10 shows the effect of the mixture of the partially oxidized $TaC_{0.58}N_{0.42}$ (DOO = 0.43) with carbon black on the potential–current curves under N_2 and O_2. In the case of only partially oxidized powder on the glassy carbon, as shown in Fig. 10a, although the ORR current was observed above 0.8 V, the ORR current was small. A larger ORR current was observed on the mixture of the partially oxidized $TaC_{0.58}N_{0.42}$ and carbon black, as shown in Fig. 10b. Upon comparison at 0.6 V, the ORR current on the mixed catalyst was 60 times larger than that on the only partially oxidized $TaC_{0.58}N_{0.42}$. However, the onset potential of each specimen was almost the same. This result suggested that the partially oxidized $TaC_{0.58}N_{0.42}$ (DOO = 0.43) had a definite catalytic activity, and the mixture with the carbon black was useful to increase the ORR current. Therefore, the mixture with the carbon black increased the surface area which acted on the active sites of the electrocatalyst because of the contact between the partially oxidized $TaC_{0.58}N_{0.42}$ and the carbon black, which had a sufficient electrical conductivity. This result indicates that the active sites of the partially oxidized $TaC_{0.58}N_{0.42}$ must have sufficient contact with the electrical conductor to obtain large ORR current.

Figure 11 shows the effect of DOO on the potential–current curves for the ORR using a mixture of the partially oxidized $TaC_{0.58}N_{0.42}$ with the carbon black catalyst. The ORR current increased with increasing DOO up to 0.43 and then decreased. The starting material (DOO = 0) and the completely oxidized material

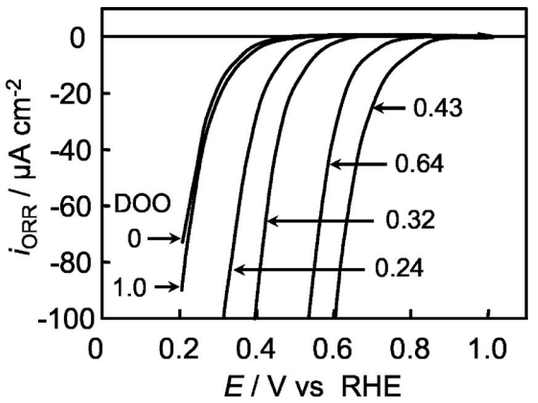

Figure 11. Effect of DOO on the potential–current curves of $TaC_{0.58}N_{0.42}$ with various DOO for the ORR in 0.1 mol dm^{-3} H_2SO_4 at 30°C. Scan rate: 5 mV s^{-1}.

(DOO = 1) had a poor catalytic activity. This result agreed with that of the partially oxidized $TaC_{0.58}N_{0.42}$ on Ti plate. Both results revealed that the partial oxidation was required to enhance the catalytic activity for the ORR. Although the titanium plate was not used to prepare the working electrode, the ORR current was observed at high potential. Therefore, the partial oxidation of the $TaC_{0.58}N_{0.42}$ was essential to have a definite catalytic activity for the ORR, indicating that carbon is much better at improving ORR activity compared to titanium. Compared to Fig. 3, the ORR current on the partially oxidized $TaC_{0.58}N_{0.42}$ mixed with carbon black on the glassy carbon rod was much larger than that on the partially oxidized $TaC_{0.58}N_{0.42}$ on the Ti plate. This result indicates that the preparation method using the mixture of partially oxidized $TaC_{0.58}N_{0.42}$ with carbon black was superior to that using electrophoretic deposition to obtain a large ORR current.

Figure 12 shows the relationship between DOO and onset potential for the ORR. The onset potential abruptly increased with increasing DOO up to 0.43. The onset potential had a maximum value of 0.83 V at a DOO of 0.43. This result revealed that relative oxidation was necessary to have a clear catalytic activity. Although the onset potential decreased with increasing DOO above 0.43, the tendency of the decrease was gradual compared to that of the increase up to 0.43. Therefore, the specimens with the DOO from 0.43 to approximately 0.7 had a clear catalytic activity for the ORR. This result indicated that a relatively wide range of partial oxidation was

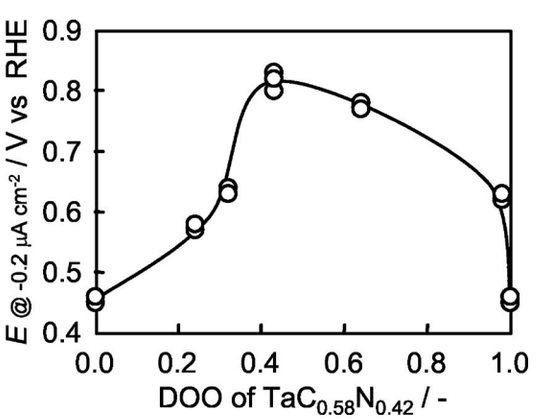

Figure 12. Relationship between the degree of oxidation of $TaC_{0.58}N_{0.42}$ and E at −0.2 μA cm^{-2}.

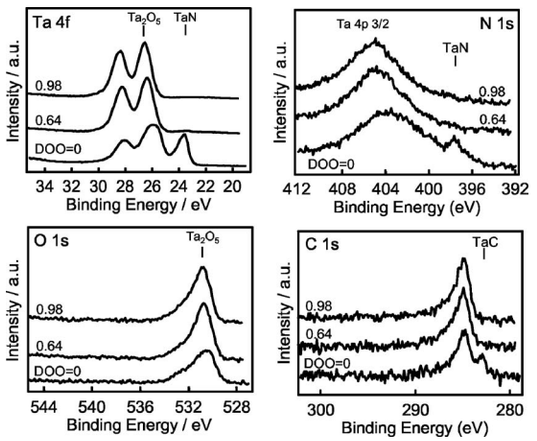

Figure 13. XPS of Ta 4f, O 1s, N 1s, and C 1s, on partially oxidized $TaC_{0.58}N_{0.42}$ with a DOO of 0, 0.64, and 0.98.

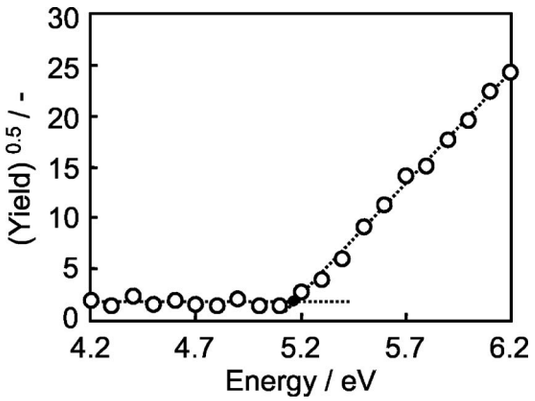

Figure 14. Relationship between the square root of the electron yield and the electron energy of partially oxidized $TaC_{0.58}N_{0.42}$ with a DOO of 0.42.

useful to enhance the catalytic activity. In addition, an appropriate oxidation of $TaC_{0.58}N_{0.42}$ is essential to have a definite catalytic activity for the ORR.

Comparing Fig. 4 and Fig. 12, the E_{ORR} showed similar dependence. Higher heat-treatment temperature of the $TaC_{0.58}N_{0.42}$/Ti corresponded to a higher DOO. Therefore, decrease in E_{ORR} above the heat-treatment temperature of 1000°C in Fig. 4 was responsible not for the formation of a nonconducting layer such as TiO_2 but the higher DOO.

Our previous study revealed that Ta–C–N thin film prepared with reactive sputtering with heat-treatment had a definite catalytic activity for the ORR.[29] The main phase of the Ta–C–N thin film was amorphous because Ta compounds were difficult to crystallize, even though the substrate was heat-treated at 800°C during film formation. Therefore, the XRD peaks of the thin film were difficult to identify because the peaks were broad and TaC (JCPDS: 35-0801), TaN (JCPDS: 09-0257), TaON (JCPDS: 20-1235), and C (JCPDS: 20-0258, 22-1069) had similar peaks. However, the results obtained in the present study suggested that the film catalyst probably included the oxygen species.

XPS was performed on the specimens with the DOO of 0, 0.64, and 0.98. Figure 13 shows the XPS of Ta 4f, O 1s, N 1s, and C 1s. In the spectrum of the Ta 4f, the Ta $4f_{7/2}$ peaks of TaN, 23.5 eV,[39] and Ta_2O_5, 26.7 eV,[40] were observed in the starting material. In addition, the peaks attributed to TaN, 397.6 eV,[41] and TaC, 282.6 eV, were observed in the spectrums of the N 1s and C 1s. Although the XRD pattern of $TaC_{0.58}N_{0.42}$ was observed in this material, the surface of the $TaC_{0.58}N_{0.42}$ particles was partially oxidized and/or oxygen molecules adsorbed on the surface.

No peaks attributed to the carbonitride were observed on the specimens with DOO of 0.64 and 0.98. From the Ta $4f_{7/2}$ and O 1s peaks, only Ta_2O_5 was detected on their surfaces. Little difference was observed between these specimens in the XPS. The surfaces of these heat-treated specimens were completely oxidized, even though both TaC_xN_y and Ta_2O_5 peaks were observed in the XRD patterns of these specimens. Therefore, these specimens were not a mixture of tantalum carbonitride with the oxide. XPS and XRD analyses indicated that the surfaces were oxidized, although the inner parts of the specimens with the DOO of 0.64 and 0.98 remained tantalum carbonitride.

Little difference was observed on the partially oxidized $TaC_{0.58}N_{0.42}$ with different DOO in the XPS analysis. Therefore, the ionization potential of the specimen was measured using a photoelectron spectrometer surface analyzer to discuss the electronic structure of the specimen. Figure 14 shows the relationship between the square root of the photoelectric quantum yield $Y^{1/2}$ and the photon energy, that is, the photoelectron spectra of the partially oxidized $TaC_{0.58}N_{0.42}$ with the DOO of 0.42. A linear relation was obtained in the range from 5.2 to 6.2 eV. The intersection between the straight line and the background line provided a threshold energy. The threshold energy corresponded to a photoelectric ionization potential. The ionization potential of the partially oxidized $TaC_{0.58}N_{0.42}$ with a DOO of 0.42 was estimated to be 5.19 eV, as shown in Fig. 14. The highest energy level of electrons in the valence band of the Ta_2O_5 is −7.8 to −7.93 eV,[32] that is, the ionization potential of Ta_2O_5 is 7.83–7.93 eV. However, the ionization potential of the partially oxidized $TaC_{0.58}N_{0.42}$ with a DOO of 0.42 was no less than 2.74 eV lower than that of Ta_2O_5. The work function of metal Ta was 4.25 eV.[42] For titanium, Henrich et al. investigated the relationship between the work function, that is, the ionization potential, of reduced TiO_2 (110) and the density of defect states on the surface.[43] They found that the work function decreased with increasing the density of defects. Similar behavior is expected to occur in the case of the partially oxidized $TaC_{0.58}N_{0.42}$. Ta_2O_5 had a bandgap of 3.9 eV.[32] Lattice defects and impurities introduce localized electron levels in the bandgap of the metal oxides. Vacancies of oxide ions give donor levels close to the edge level of the conduction band.[44] The conduction band edge level of Ta_2O_5 is −3.93 to −4.03 eV.[32] These values are close to the ionization potential of partially oxidized $TaC_{0.58}N_{0.42}$, with a DOO of 0.42. Therefore, the partially oxidized $TaC_{0.58}N_{0.42}$ with a DOO of 0.42 probably had some oxide ion vacancies.

The adsorption of oxygen molecules on the surface was required as the first step to proceed with the ORR. Many researches revealed that the presence of surface defects sites was required to adsorb the oxygen molecules on the surface of the oxides, such as TiO_2 (110), ZnO, NiO(100), $Ce_xZr_{(1-x)}O_2$, V_2O_5, and MoO_3.[45-50] Therefore, the increase in the surface defects on the partially oxidized $TaC_{0.58}N_{0.42}$ yielded the increase in the adsorption sites of oxygen molecules. In addition, interaction of oxygen with the catalyst surface is essentially important, because both the adsorption of oxygen and the desorption of water on the surface is necessary to continue fluent progression of the ORR. When the interaction of oxygen with the catalyst surface is strong, the desorption of water is restrained. When the interaction of oxygen with the catalyst surface is weak, little adsorption of oxygen molecules proceeds. Therefore, there exists a suitable strength of interaction between the oxygen and the catalyst surface. Metal Ta strongly adsorbed oxygen because of the large adsorption energy of oxygen (887 kJ mol^{-1}) and calculated bond energy of Ta–oxygen atoms (715 kJ mol^{-1}).[51] In the case of Pt, the adsorption energy of oxygen and the calculated bond energy of Pt–oxygen atoms were 280 kJ mol^{-1} and 397 kJ mol^{-1}, respectively.[51] Therefore, these Ta values were much larger than those of Pt. As the oxidization of metal Ta proceeded, the interaction of oxygen with Ta of the catalyst surface became weak because the

oxide ions attracted the electrons of the highest occupied molecule orbital of Ta to be positively charged Ta. Therefore, the oxidization could control the strength of the interaction between the oxygen and the Ta, and as the interaction became suitable the catalytic activity for the ORR increased. Further investigation is required to clarify the effect of the crystalline structure as well as the surface defects of the partially oxidized $TaC_{0.58}N_{0.42}$ on the catalytic activity of the ORR.

Conclusions

Partially oxidized $TaC_{0.58}N_{0.42}$ was investigated as a cathode for PEFCs. The working electrodes were prepared by two methods. First, the working electrode was prepared by electrophoretic deposition of the $TaC_{0.58}N_{0.42}$ powder on the Ti substrate. Then the $TaC_{0.58}N_{0.42}$/Ti was heat-treated under flowing nitrogen/hydrogen gas (H_2:2%) with 0.25% oxygen. The $TaC_{0.58}N_{0.42}$ on the Ti plate was partially oxidized during heat-treatment. Second, the $TaC_{0.58}N_{0.42}$ powder was partially oxidized by the heat-treatment under flowing nitrogen/hydrogen gas (H_2:2%) with 0.25% oxygen mixed with carbon black to obtain a sufficient electrical contact. In both cases, the catalytic activity of the ORR depended significantly on the partial oxidation state of the $TaC_{0.58}N_{0.42}$. The XRD analysis showed that both TaC_xN_y and Ta_2O_5 peaks were observed in the specimens, which had a definite catalytic activity for the ORR. XPS analysis revealed that the surface of the heat-treated specimens was completely oxidized to Ta_2O_5, even though the catalytic activity was different among the heat-treated specimens. The ionization potential measurement suggested that the partially oxidized $TaC_{0.58}N_{0.42}$ with some defects on the surface had a definite catalytic activity for the ORR. We think that there is an ideal strength of interaction between the oxygen and Ta on the catalyst surface. The interaction was probably affected by the oxidization of Ta, and as the interaction became suitable the catalytic activity for the ORR increased.

Acknowledgments

The authors thank A.L.M.T. Corporation for supply of the $TaC_{0.58}N_{0.42}$ and Riken Keiki Co., Limited, for measurement of the ionization potential. The authors also thank the New Energy and Industrial Technology Development Organization (NEDO) for financial support.

Yokohama National University assisted in meeting the publication costs of this article.

References

1. A. Ishihara, S. Mitsushima, N. Kamiya, and K. Ota, *J. Power Sources*, **126**, 34 (2004).
2. D. M. Bernardi and M. W. Verbrugge, *J. Electrochem. Soc.*, **139**, 2477 (1992).
3. Metal Economics Research Institute, Japan, *Report on Trends for the Supply and Demand of Platinum Group Metals for Fuel Cell Systems*, pp. 38 and 351 (2005), in Japanese.
4. Japan Automobile Manufactures Association, Inc., *The Motor Industry of Japan 2005*, p. 42 (2005).
5. R. Jasinski, *Nature (London)*, **201**, 1212 (1964).
6. H. Jahnke and M. Schönborn, *Comptes Rendus, Troisièmes Journées Internationales d'Etude des Piles à Combustible, 60*, Presses Académiques Européennes, Bruxelles (1969).
7. J. H. Zagal, *Coord. Chem. Rev.*, **119**, 89 (1992).
8. K. Shigehara and F. C. Anson, *J. Phys. Chem.*, **86**, 2776 (1982).
9. J. P. Collman, P. S. Wagenecht, and J. E. Hutchison, *Angew. Chem. Int. Ed. Engl.*, **33**, 1537 (1994).
10. H. Jahnke, M. Schönborn, and G. Zimmermann, *Top. Curr. Chem.*, **61**, 133 (1976).
11. E. Yeager, *Electrochim. Acta*, **29**, 1527 (1984).
12. D. A. Scherson, A. A. Tanaka, S. L. Gupta, D. Tryk, C. Fierro, R. Holze, E. B. Yeager, and R. P. Lattimer, *Electrochim. Acta*, **31**, 1247 (1986).
13. A. Van der Putten, A. Elzing, W. Visscher, and E. Barendrecht, *J. Electroanal. Chem. Interfacial Electrochem.*, **221**, 95 (1987).
14. A. Van der Putten, A. Elzing, W. Visscher, and E. Barendrecht, *J. Electroanal. Chem. Interfacial Electrochem.*, **205**, 233 (1986).
15. J. A. R. Van Veen, H. A. Colijn, and J. F. Van Baar, *Electrochim. Acta*, **33**, 801 (1988).
16. A. L. Bouwkamp-Wijnoltz, W. Visscher, J. A. R. Van Veen, and S. C. Tang, *Electrochim. Acta*, **45**, 379 (1999).
17. G. Gruenig and K. Wiesener, *J. Electroanal. Chem. Interfacial Electrochem.*, **159**, 155 (1983).
18. K. Wiesener, *Electrochim. Acta*, **31**, 1073 (1986).
19. N. Alonso-Vante and H. Tributsch, *Nature (London)*, **323**, 431 (1986).
20. N. Alonso-Vante, in *Handbook of Fuel Cells—Fundamentals, Technology and Applications*, Vol. 2, W. Vielstich, A. Lamm, and H. A. Gasteiger, Editors, pp. 534–543, John Wiley & Sons, Ltd., West Sussex (2003).
21. K. Lee, A. Ishihara, S. Mitsushima, N. Kamiya, and K. Ota, *Electrochim. Acta*, **49**, 3479 (2004).
22. A. Ishihara, K. Lee, S. Doi, S. Mitsushima, N. Kamiya, M. Hara, K. Domen, K. Fukuda, and K. Ota, *Electrochem. Solid-State Lett.*, **8**, A201 (2005).
23. Y. Shibata, A. Ishihara, S. Mitsushima, N. Kamiya, and K. Ota, *Electrochem. Solid-State Lett.*, **10**, B43 (2007).
24. Y. Liu, A. Ishihara, S. Mitsushima, N. Kamiya, and K. Ota, *Electrochem. Solid-State Lett.*, **8**, A400 (2005).
25. Y. Liu, A. Ishihara, S. Mitsushima, N. Kamiya, and K. Ota, *J. Electrochem. Soc.*, **154**, B664 (2007).
26. J.-H. Kim, A. Ishihara, S. Mitsushima, N. Kamiya, and K. Ota, *Electrochim. Acta*, **52**, 2492 (2007).
27. S. Doi, A. Ishihara, S. Mitsushima, N. Kamiya, and K. Ota, *J. Electrochem. Soc.*, **154**, B362 (2007).
28. J.-H. Kim, A. Ishihara, S. Mitsushima, N. Kamiya, and K. Ota, *Chem. Lett. (Jpn.)*, **36**, 514 (2007).
29. J.-H. Kim, A. Ishihara, S. Mitsushima, N. Kamiya, and K. Ota, *Electrochemistry (Tokyo, Jpn.)*, **75**, 166 (2007).
30. J. W. Schultze and A. W. Hassel, in *Encyclopedia of Electrochemistry*, Vol. 4, M. Stratmann and G. S. Frankel, Editors, p. 234, Wiley-VCH, Weinheim (2003).
31. N. Sato, *Electrochemistry at Metal and Semiconductor Electrodes*, Chap. 8, ElsevierScience B. V, Amsterdam (1998).
32. W.-J. Chun, A. Ishikawa, H. Fujisawa, T. Takata, J. N. Kondo, M. Hara, M. Kawai, Y. Matsumoto, and K. Domen, *J. Phys. Chem. B*, **107**, 1798 (2003).
33. H. O. Pierson, *Handbook of Refractory Carbides and Nitrides*, p. 87, Noyes Publications, Park Ridge, NJ (1996).
34. H. Ihara, M. Hirabayashi, and H. Nakagawa, *Phys. Rev. B*, **14**, 1707 (1976).
35. D. A. Papaconstantopoulos, W. E. Pickett, B. M. Klein, and L. L. Boyer, *Phys. Rev. B*, **31**, 752 (1985).
36. O. Yu. Khyzhun and V. A. Kolyagin, *J. Alloys Compd.*, **363**, 32 (2004).
37. N. Koura, T. Tsukamoto, H. Shoji, and T. Hotta, *J. Appl. Phys.*, **34**, 1643 (1995).
38. H. Kirihata and M. Uda, *Rev. Sci. Instrum.*, **52**, 68 (1981).
39. L. Shi, Z. Yang, L. Chen, and Y. Qian, *Solid State Commun.*, **133**, 117 (2005).
40. J. F. Moulder, W. F. Sticle, P. E. Sobol, and K. D. Bomben, in *Handbook of X-ray Photoelectron Spectroscopy*, J. Chastain and R. C. King, Jr., Editors, Physical Electronics, Inc., Eden Prairie, MN (1995).
41. E. R. Engbrecht, Y.-M. Sun, S. Smith, K. Pfiefer, J. Bennett, J. M. White, and J. G. Ekerdt, *Thin Solid Films*, **418**, 145 (2002).
42. H. B. Michaelson, *J. Appl. Phys.*, **48**, 4729 (1977).
43. V. E. Henrich, G. Dresselhaus, and H. J. Zeiger, *Phys. Rev. Lett.*, **36**, 1335 (1976).
44. C. Stampfl and A. J. Freeman, *Phys. Rev. B*, **67**, 064108 (2003).
45. J.-M. Pan, B. L. Maschhoff, U. Diebold, and T. E. Madey, *J. Vac. Sci. Technol. A*, **10**, 2470 (1992).
46. A. L. Lisebigler, G. Lu, and J. T. Yates, Jr., *Chem. Rev. (Washington, D.C.)*, **95**, 735 (1995).
47. C. Descorme, Y. Madier, and D. Duprez, *J. Catal.*, **196**, 167 (2000).
48. J. M. Blaisdell and A. B. Kunz, *Phys. Rev. B*, **29**, 988 (1984).
49. W. Göpel, *J. Vac. Sci. Technol.*, **15**, 1298 (1978).
50. M. Witko and R. Tokarz-Sobieraj, *Catal. Today*, **91–92**, 171 (2004).
51. E. Miyazaki and I. Yasumori, *Surf. Sci.*, **55**, 747 (1976).